$SiO_2(200)$ than for $SiO_2(500)$.[7,24]

The same surface species, $\equiv SiOSnR_3$, is obtained already at ambient temperature by reaction 2 between Bu_3SnH and the silanol groups, suggesting that a Sn-H bond is more reactive toward silanol groups than a Sn-C bond. The thermal stability

$$\equiv SiOH + HSnBu_3 \rightarrow \equiv SiO\text{-}SnBu_3 + H_2 \qquad (2)$$

of these surface grafted trialkyltin complexes is slightly higher on the surface of a silica dehydroxylated at 500 °C than on a more hydroxylated surface, such as $SiO_2(200)$ for example. On the latter surface, reaction with neighboring available OH groups takes place.[13] The overall reactivity of SnR_4 and $HSnR_3$ complexes is summarized in Scheme I.

Conclusion

The reaction between a number of tetraalkyltin or hydridotributyltin complexes and the surface of partially dehydroxylated silica leads to the clean formation of the related trialkyltin surface complexes, $\equiv SiOSnR_3$, with liberation of 1 mol of alkane or 1 mol of H_2, respectively, per mol of surface tin. The alkyl ligands are interacting with the surface silanol groups via hydrogen-type bonds. This interaction occurs when surface hydroxyl groups are available and accessible, when the hydrocarbon chain length is sufficient, and when the temperature is lower than 80 °C. These surface organometallic SnR_3 fragments are stable up to at least 200 °C, when the surface of silica was previously dehydroxylated at 500 °C. This described chemistry has recently been extrapolated to the external surface of a mordenite: the SnR_3 entities are able to induce new shape selective properties for the zeolite.[27]

(27) Nédez, C.; Theolier, A.; Choplin, A.; Basset, J. M.; Joly, J. F.; Benazzi, E. To be published.
(28) Bishop, M. E.; Schaeffer, C. D.; Zuckerman, J. J. *J. Organomet. Chem.* **1975**, *101*, C19.

Oxidative Coupling and Ring Opening of Furan on Ag(110): Formation of Maleic Anhydride, Benzene, and Bifuran

William W. Crew and Robert J. Madix*

Contribution from the Department of Chemical Engineering, Stanford University, Stanford, California 94305. *Received July 3, 1992*

Abstract: TPRS, EELS, and isotope experiments show that furan reacts with active oxygen on Ag(110) to form CO_2, H_2O, and small amounts of the partially oxidized products maleic anhydride, bifuran, and benzene that evolve between 520 and 560 K. The first step in furan combustion is C-H bond activation by $O_{(a)}$, followed by $O_{(a)}$ attack at the α-carbon at 308 K. $^{18}O_{(a)}$ experiments prove that maleic anhydride is formed via intermediates where the furan ring has been cleaved. This contrasts with mechanisms proposed for maleic anhydride production from furan over VPO catalysts.

Introduction

Silver catalysts are used for the industrial epoxidation of ethylene to ethylene epoxide. Although much is still not known about this industrially significant reaction, the behavior of oxygen on Ag(110) is quite well understood. Atomic oxygen behaves as a Brönsted base, exemplified in the observed acid-base reaction of atomic oxygen and adsorbed formic acid:[1]

$$HCOOH_{(a)} + O_{(a)} \rightarrow HO_{(a)} + HCOO_{(a)} \qquad (1)$$

Adsorbed atomic oxygen also behaves as a nucleophile, attacking electron-deficient carbon centers, as in the observed reaction of atomic oxygen and formaldehyde:[1]

$$H_2CO_{(a)} + O_{(a)} \rightarrow H_2CO_{2(a)} \qquad (2)$$

The fact that oxygen behaves both as a Brönsted base and as a nucleophile implies that adsorbed oxygen is partly anionic. Experimental and theoretical evidence confirms this observation.[2-4]

Reactions on Ag(110) of oxygen with unsaturated hydrocarbons can be classified as C-H bond activation, C=C epoxidation, and cycloaddition. Although C-H bond activation by $O_{(a)}$ has been known for some time, epoxidation reactions by this species were confirmed only recently with the epoxidation of both norbornene to norbornene epoxide[5] and 3,3-dimethyl-1-butene to 3,3-dimethyl-1-butene epoxide.[6] Even more recently, Roberts et al. observed the cycloaddition of 1,3-butadiene with $O_{(a)}$ to form 2,5-dihydrofuran.[7]

The activation of C-H bonds by atomic oxygen on silver is governed by the gas-phase acidity or heterolytic bond dissociation enthalpy (ΔH_{acid}), determined by the following gas-phase reaction:

$$R\text{-}H \rightarrow R^+ + H^- \qquad (\Delta H = \Delta H_{acid}) \qquad (3)$$

If the heterolytic bond dissociation enthalpy of the conjugate base is less than that of water (ΔH_{acid} = 395 kcal/mol), then the following acid-base reaction is expected to occur:

$$BH_{(a)} + O_{(a)}^- \rightarrow B_{(a)}^- + HO_{(a)} \qquad (4)$$

Hence, propylene (ΔH_{acid} = 392 kcal/mol[8]) reacts with $O_{(a)}$ to form surface hydroxyl groups and, at higher temperatures, CO_2 and H_2O; cyclohexene (ΔH_{acid} = 387 kcal/mol[9]) reacts with surface oxygen to yield benzene.[10]

Recently, 1-butene was observed to react with surface oxygen to yield butadiene, 2,5-dihydrofuran, furan, 2(5*H*)-furanone, and maleic anhydride.[11] The following mechanism was proposed. First, 1-butene acidic C-H bond activation by $O_{(a)}$ leads to butadiene formation. Butadiene and oxygen undergo 1,4-cycloaddition to form 2,5-dihydrofuran. 2,5-Dihydrofuran is acidic

* To whom correspondence should be addressed.

(1) Barteau, M. A.; Bowker, M.; Madix, R. J. *Surf. Sci.* **1980**, *94*, 303.
(2) Madix, R. J.; Solomon, J. L.; Stöhr, J. *Surf. Sci.* **1988**, *197*, L253.
(3) Barteau, M. A.; Madix, R. J. *J. Electron Spectrosc. Relat. Phenom.* **1983**, *31*, 101.
(4) Wurth, W.; Stöhr, J., unpublished results.
(5) Roberts, J. T.; Madix, R. J. *J. Am. Chem. Soc.* **1988**, *110*, 8540.
(6) Mukoid, C.; Hawker, S.; Badyal, J. P. S.; Lambert, R. M. *Catal. Lett.* **1990**, *4*, 57.
(7) Roberts, J. T.; Capote, A. J.; Madix, R. J. *J. Am. Chem. Soc.* **1991**, *113*, 9848.
(8) DePuy, C. H.; Bierbaum, V. M.; Damraurer, R. *J. Am. Chem. Soc.* **1984**, *106*, 4051.
(9) Lee, R. E.; Squires, R. R. *J. Am. Chem. Soc.* **1986**, *108*, 5078.
(10) Roberts, J. T.; Madix, R. J. *Surf. Sci.* **1990**, *226*, L71.
(11) Roberts, J. T.; Capote, A. J.; Madix, R. J. *Surf. Sci.* **1991**, *253*, 13.

0002-7863/93/1515-729$04.00/0

enough to undergo C–H bond activation by $O_{(a)}$ to form furan. Further oxidation of furan yields 2(5*H*)-furanone and maleic anhydride. The latter reaction could occur by oxygen addition to furan.

In this work we investigated the oxidation pathway of furan in order to better understand both the reaction pathway for maleic anhydride production from 1-butene on Ag(110) and, more generally, the reactivity of aromatic compounds with $O_{(a)}$. Although furan is aromatic, it reacts readily with atomic oxygen. Indeed, furan is sufficiently acidic (ΔH_{acid} = 388 kcal/mol)[12] to undergo C–H bond activation by $O_{(a)}$, and C–H bond activation is the first step in furan oxidation. Furan then undergoes further oxidation to form complete combustion products CO_2 and H_2O and small amounts of maleic anhydride, bifuran, furan, and benzene. Product yields show that complete combustion of furan is highly favored over production of partially oxidized products. In addition, isotope experiments prove that maleic anhydride is formed via intermediates where the furan ring is opened. This result contrasts with the proposed mechanism for maleic anhydride formation from furan over V_2O_5/P_2O_5 catalysts.[13]

Experimental Section

Experiments were performed in three different stainless steel, ultra-high-vacuum chambers using three different Ag(110) crystals. The three chambers are described in detail elsewhere.[14-16] Electron energy loss spectroscopy (EELS) was performed in one chamber, and temperature-programmed reaction spectroscopy (TPRS) was performed in the other two. The surface chemistry was reproduced on all three crystals using TPRS experiments. The operating base pressure of the chambers was $\approx(1-2) \times 10^{-10}$ Torr. All chambers possessed the capability to cool the crystal to 100 K by thermal conduction through crystal support rods to a hollow copper block containing liquid nitrogen. All three crystals, between 15 and 20 mm in diameter, were held by a tantalum wrap spot welded to support wires. Crystal heating in the EELS chamber and a TPRS chamber was achieved by resistive heating. The third crystal was heated by electron bombardment. The Ag(110) crystals were cleaned by repeated cycles of Ar^+ ion bombardment, and then they were annealed to 700 K. Surface cleanliness was verified by Auger electron spectroscopy. Carbon impurities were removed by oxygen titration until the CO_2 desorption yield was less than 1% of the $O_{2(g)}$ yield for a given exposure of oxygen. Surface oxygen coverages were calibrated by comparing oxygen desorption yields to that observed for 0.5 mL of $O_{(a)}$, the saturation coverage on Ag(110).

TPRS experiments were conducted on all three chambers. All chambers were equipped with a UTI 100C quadrupole mass spectrometer interfaced to an IBM XT or compatible microcomputer. All mass spectrometer ionization cages were fitted with a glass cap with an orifice approximately 3 mm in diameter in the front of the cap, on axis with the quadrupoles. Preferential detection of products desorbing from the center of the crystal was achieved by placing the crystal less than 5 mm from the cap orifice. Initial TPRS experiments were performed using a program capable of analyzing up to 150 ions per experiment but at the expense of temperature resolution.[17] After it was determined which ions were present, 10 ions per TPRS experiment were used for product identification and determination of detailed desorption characteristics with increased resolution in the TPRS traces. For all TPRS experiments a heating rate of 5 K/s was observed up to 750 K.

EELS spectra were recorded using an LK-2000 high-resolution electron energy loss spectrometer. Spectra for these experiments were taken with the beam energy of ≈5 eV with a resolution of 8 meV at a crystal temperature of 100 K. Count rates for furan on a clean Ag(110) surface were 5×10^5 Hz, and those of adsorbate-covered, annealed surfaces were approximately 3×10^4 Hz. Annealed surfaces were quickly heated to the desired temperature and then cooled to 100 K before an EELS spectrum was taken.

Compounds were purchased from Aldrich, Matheson Gas Products, or Cambridge Isotope Laboratories (CIL). Furan (Aldrich, 99+%), furan-d_4 (Aldrich, 99%-*d*), maleic anhydride (Aldrich, 99%), oxygen (Matheson, extra dry, 99.6% minimum), $^{18}O_2$ (CIL, 97.7% ^{18}O), and argon (Matheson, prepurified 99.998%) were used without further purification. By leaking ^{18}O into the chamber and monitoring all the possible O_2 isotopes, we determined the ^{18}O purity to be 98.7%. Liquid samples were degassed prior to use by freeze–pump–thaw cycles until the vapor pressure observed over the solid phase was below the limit of detectability, 1×10^{-3} Torr.

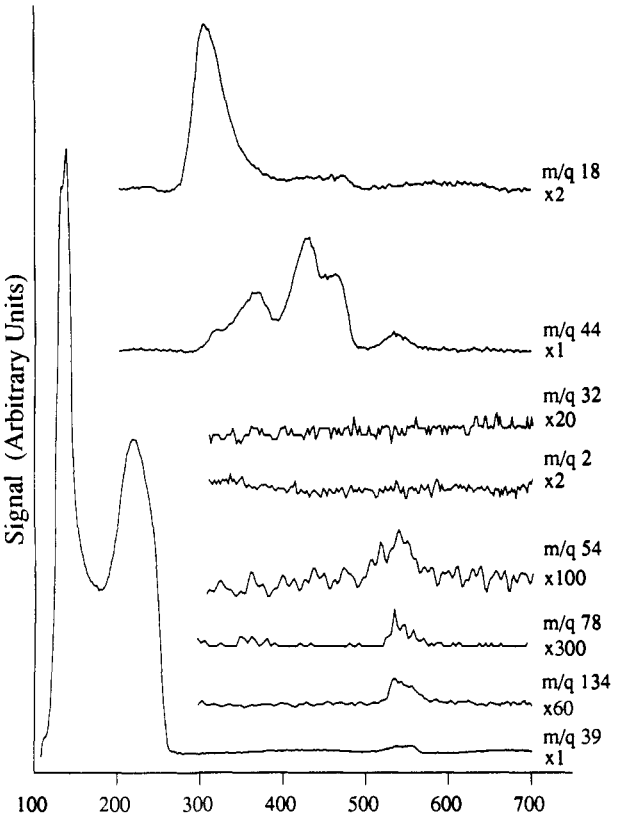

Figure 1. TPRS of multilayer furan on Ag(110) precovered with 0.25 ML of $O_{(a)}$. Traces of partial oxidation products were taken separately on a higher mass spectrometer sensitivity.

Results

Temperature-programmed reaction spectra for furan absorbed on an Ag(110) surface precovered with 0.25 monolayer (ML) of $O_{(a)}$ are shown in Figure 1. Unreacted furan (m/q 39) desorbs molecularly from the surface by 250 K. Primary products from the reaction of furan with adsorbed atomic oxygen are CO_2 (m/q 44) and H_2O (m/q 18). Maleic anhydride (m/q 54), benzene (m/q 78), bifuran (m/q 134, the parent ion), and reaction-limited furan evolve into the gas phase in small quantities between 520 and 560 K and are attributed to the incomplete oxidation of furan. In addition to these known products, a product of m/q 92 was observed with the stoichiometry C_6H_4O and is tentatively assigned to either benzoquinone or benzofuran. Products were identified by comparing mass ion yields of known compounds leaked into the chamber with those from TPRS experiments and by monitoring product mass ion shifts from ^{18}O and furan-d_4 isotope experiments to determine the number of oxygen and hydrogen atoms in each species.

Furan (m/q 39) desorbs in three states, 120, 220, and 520 K. For all three states the cracking patterns agree with those for furan samples leaked into the chamber. In addition, furan-d_4 experiments showed a parent mass ion shift from m/q 68 to 72; ^{18}O experiments showed no mass ion shift, indicating that no surface oxygen was incorporated into the desorbing species. The 120 K desorption peak does not saturate with increasing furan exposures and is therefore attributed to furan desorption from the multilayer. Because furan monolayer desorption occurs at 180 K on the clean surface, the broad desorption feature at 220 K is assigned to furan desorption from silver stabilized by $O_{(a)}$. The 530 K peak is well above the molecular desorption temperature of furan and is therefore attributed to reaction-limited evolution of furan.

Primary reaction products are water and carbon dioxide, indicating that combustion is highly favored over the formation of

(12) DePuy, C. H.; Kass, S. R.; Bean, G. P. *J. Org. Chem.* **1988**, *53*, 4427.
(13) Do, N. T.; Baerns, M. *Appl. Catal.* **1988**, *45*, 9.
(14) Solomon, J. L.; Madix, R. J.; Stöhr, J. *J. Chem. Phys.* **1991**, *94*, 4012.
(15) Stuve, E. M.; Madix, R. J. *Surf. Sci.* **1985**, *160*, 293.
(16) Capote, A. J.; Madix, R. J. *J. Am. Chem. Soc.* **1989**, *111*, 3570.
(17) Liu, A. C.; Friend, C. M. *Rev. Sci. Instrum.* **1986**, *57*, 1519.

other partially oxidized products. Water desorbs in a peak at 300 K and a broad feature from 350 to 480 K. Water from the 300 K state results from surface hydroxyl ($OH_{(a)}$) disproportionation—the presence of hydroxyl groups was verified by EELS, as discussed below.[18,19] Other high-temperature product states result from further oxidation of adsorbed hydrocarbon fragments resulting from reactions of furan. Carbon dioxide evolves in reaction channels at 320, 370, 430, 460, and 530 K. All carbon dioxide results from the attack of surface atomic oxygen on chemisorbed furan or partially combusted furan fragments. The 320 K channel results from the initial attack of surface oxygen ($O_{(a)}$) on surface-bound furan intermediates; the 370 K pathway results from continued oxidation of furan rings; the 430 and 460 K channels result from oxidation of more furan rings and hydrocarbon fragments (see below). Carbon dioxide evolution at 530 K is similar to that of the products benzene, maleic anhydride, bifuran, and furan. The concurrent evolution of both partial and complete oxidation products implies that complete combustion of product precursors competes with product formation.

Maleic anhydride formation at 530 K was verified by both mass ion yield analysis and isotope experiments. The yield ratio between m/q 98, the parent ion, and m/q 54 for the furan TPRS experiment is 1:30, the same ratio observed for maleic anhydride leaked into the chamber. In addition, TPRS experiments of furan-d_4 on oxygen-precovered Ag(110) show a parent ion mass shift of 2 amu, indicating that the product has two hydrogens. TPRS experiments of furan on ^{18}O-precovered Ag(110) show a parent ion mass shift of 4 amu, indicating that two surface oxygens are present in the product. These mass shifts agree with those expected for maleic anhydride production. Further, m/q 98 was identified as the parent ion because no other products were observed on the highest mass spectrometer settings for 98–150 amu with the same kinetics.

Benzene was identified by the same TPRS peak shapes for major ion fractions of benzene: m/q 78 (C_6H_6), 77 (C_6H_5), and 52 (C_4H_4). Other major ion fractions of benzene, m/q 39 (C_3H_3) and 26 (C_2H_2), are also major fractions of furan, and contributions due to benzene were obscured in the high-temperature furan desorption state. An ion mass yield analysis was not performed because at the high mass spectrometer sensitivities required to get reliable ion intensities, the large time constant of the mass spectrometer prevents sampling of more than three masses per TPRS experiment while still obtaining adequate temperature resolution. TPRS experiments using furan-d_4 show a parent ion mass shift from m/q 78 to 84, indicating that the product contains six hydrogens. Because no ion mass shift is observed for TPRS experiments using $^{18}O_{(a)}$, no surface oxygens are incorporated into the product. This does not absolutely rule out the existence of oxygen in the product, however. If the product were derived from the partial combustion of furan, it might contain ^{16}O from the furan molecule and not exhibit an ion mass shift in the $^{18}O_{(a)}$ TPRS experiments. However, because no other ion fragment with the same TPRS peak shape as m/q 78 was observed in the range m/q 79–150, m/q 78 is concluded to be the parent ion, and the only possible stoichiometry that agrees with experimental data is that of benzene, C_6H_6.

Bifuran, represented in Figure 1 by its parent ion fraction m/q 134, was identified primarily from isotope experiments. No ion mass yield calibrations were performed for bifuran. TPRS traces with the same peak shape were observed for m/q 134 and 105. For furan the two most abundant ion mass fragments are CHO (m/q 29) and C_3H_3 (m/q 39). If bifuran underwent similar fragmentation, then it would exhibit CHO (m/q 29) and C_7H_5O (m/q 105) as major fragments. In fact, published ion fragment data for bifuran shows that m/q 134 and 105 are its major fragments.[20] Isotope experiments provide additional evidence for bifuran production. Furan-d_4 TPRS experiments with $^{16}O_{(a)}$ adsorbed on Ag(110) show an ion mass shift from m/q 134 to 140, confirming that the product contains six hydrogens. No ion mass shift is observed for TPRS experiments using ^{18}O, demonstrating that no surface oxygen atoms are incorporated into the product and that all oxygens must originate from furan. The only two stoichiometries that can satisfactorily explain these experimental results are $C_8H_6O_2$ (bifuran) and $C_4H_6O_5$. Although two stoichiometries exist, the latter requires the incorporation of four oxygen atoms from oxygen-containing furan fragments *not* from the surface. Such a reaction seems improbable. Bifuran, however, can be made simply by joining two adsorbed furanyls (C_4H_3O-), which we believe to be formed initially by the reaction of furan with surface oxygen, as described below.

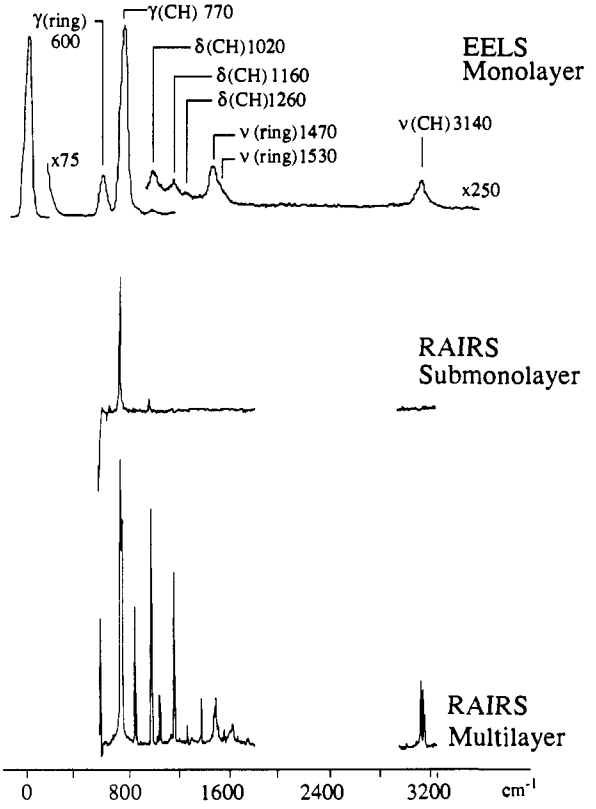

Figure 2. RAIRS and EELS spectra of furan on clean Ag(110).

EELS was used to aid in the identification of surface-bound intermediates in furan oxidation. To isolate reaction intermediates, the surface was flashed to prescribed temperatures and then cooled to 100 K for recording the spectrum. This technique isolates irreversibly formed reaction intermediates only. While EELS spectra provided information about the initial combustion process, intermediates leading to partially oxidized products were not detectible because the partial oxidation products are produced in small amounts, making detection of precursor signature vibrations difficult, and product signature modes were hidden by vibrations from other hydrocarbon fragments on the surface. After a multilayer of furan adsorbed on 0.25 mL of $O_{(a)}$ was flashed to 700 K, oxygen titration and EELS spectra of the surface show that hydrocarbon fragments remained on the surface. Nonetheless, EELS spectra provided valuable information concerning the first step in the furan combustion process and the orientation of the first intermediate formed.

Furan lies flat with its ring parallel to the surface on clean Ag(110). NEXAFS and RAIRS confirm this orientation.[14,21] To verify EELS vibration assignments for furan, energy losses were compared to published data for both furan and furan-d_4 (Table I).[21,22] The expected modes were visible in EELS for both isotopes of furan. The RAIRS and EELS spectra for furan on Ag(110)

(18) Stuve, E. M.; Madix, R. J.; Sexton, B. A. *Surf. Sci.* **1982**, *123*, 491.
(19) Barteau, M. A.; Madix, R. J. *Surf. Sci.* **1982**, *115*, 355.
(20) McLafferty, F. W.; Stauffer, D. B. *The Wiley/NBS Registry of Mass Spectral Data*; John Wiley & Sons: New York, 1989; Vol. 1.
(21) Huberty, J.; Madix, R. J., unpublished results.
(22) Rico, M.; Barrachina, M.; Orza, J. M. *J. Mol. Spectrosc.* **1967**, *24*, 133.

Table 1. Vibrational Assignments for Furan and Furan-d_4 on Ag(110)

assignment	FTIR[21] multilayer	FTIR[21] monolayer	EELS monolayer
ν CH	3153 (2338)[a] w		
ν CH	3144 (2350) m		
ν CH	3125 (2371) m		3120 (2350)[b] m
ν CH	3117 (2327) sh		
2 × 1553 = 3106	3087 vw		
1490 + 1553 = 3043	3017 vw		
869 + 755 = 1624	1617 w		
ν ring	1553 (1490) w		1530 (1480) sh
ν ring	1490 (1424) m		1470 (1400) w
ν ring	1382 (1315) m		(1280)
δ CH	1268 (1140) w		(1120)
δ CH	1162 (1054) s	1162 vw	1160 (1040) w
δ CH	1055 (920) m		1020 (910) w
δ CH	992 (791) s	987 w	(800)
δ ring	869 (727) s		860 (720) sh
γ CH	763 (597) vs	764 vs	770 (600) vs
γ ring	605 (500) s	602 w	600 (520) m

[a] Numbers in parentheses are gas-phase vibrational assignments of furan-d_4.[22] [b] Numbers in parentheses are vibrational assignments for monolayer furan-d_4 on Ag(110).

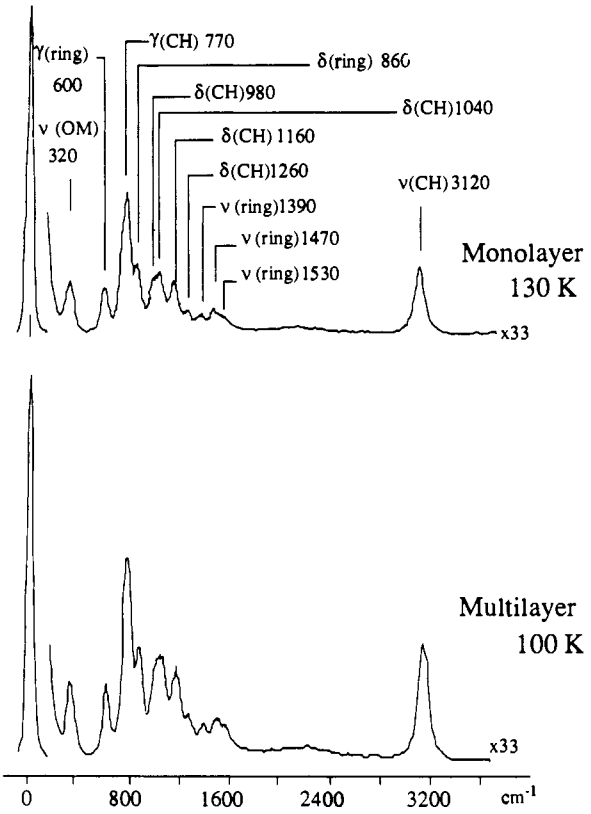

Figure 3. EELS spectra of furan on Ag(110) precovered with 0.25 ML of $O_{(a)}$.

are shown in Figure 2. RAIRS detects only dipole modes perpendicular to the surface. Several modes are detected in the randomly oriented multilayer, but only the out-of-plane modes are clearly visible in the monolayer spectrum. Because in-plane modes are screened and only the out-of-plane modes are detected in the monolayer, furan must be lying flat on the Ag(110) surface. A detailed discussion of the FTIR data will be published later.[21] Correspondingly, the EELS spectra also show strong out-of-plane and weak in-plane modes.

A monolayer of furan on an oxygen-precovered Ag(110) surface, prepared by flashing the multilayer-covered surface to 130 K, appears to be randomly oriented. Figure 3 shows EELS spectra of the furan multilayer and monolayer on Ag(110) precovered with 0.25 ML of oxygen. In these spectra, more modes are visible,

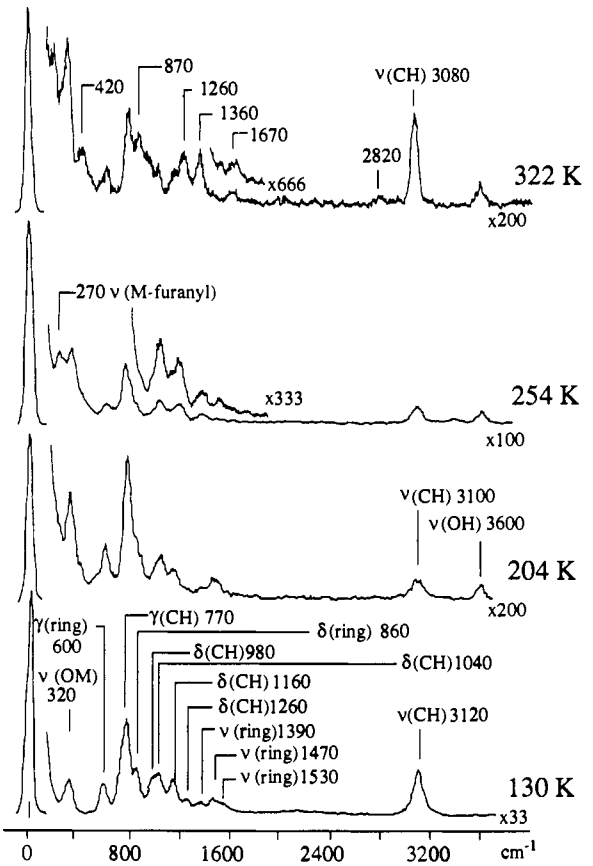

Figure 4. EELS spectra of multilayer doses of furan and 0.25 ML of $O_{(a)}$ on Ag(110), flashed to indicated temperatures and cooled to 100 K before a spectrum was taken.

the in-plane modes are stronger, and the out-of-plane modes are weaker than for the spectra of monolayer furan on clean Ag(110). There is no difference in relative loss intensities between the multilayer and monolayer spectra in Figure 3. The decrease in out-of-plane mode intensity and corresponding increase in in-plane intensity indicate that, on average, furan on the precovered surface is tilted more toward the surface normal than furan on clean Ag(110). Although this trend is expected for an EELS spectrum of a randomly oriented multilayer on Ag(110), it is somewhat surprising at monolayer furan coverages. Assuming that oxygen does not alter mode dipole moments of furan adsorbed to the surface, monolayer furan on the oxygen-precovered Ag(110) must be more tilted toward the surface normal than on the clean surface.

The first reaction in furan combustion is hydrogen abstraction by adsorbed atomic oxygen. Figure 4 shows EELS spectra of multilayer furan on Ag(110) precovered with 0.25 mL of $O_{(a)}$ and annealed to 130, 204, 254, and 322 K. The EELS spectra of the surface annealed to 204 K shows all of the modes as furan at 130 K, plus modes at 320 and 3600 cm^{-1}. The low-frequency mode is assigned to the oxygen–metal stretch (ν(M–O)).[23] The high-frequency mode agrees with published data for the oxygen–hydrogen stretch of surface hydroxyl groups (ν(O–H)),[24] indicating that hydrogen abstraction from furan occurs by 204 K.

EELS spectra also show that with a hydrogen abstracted the furan ring tilts more toward the surface normal than does furan on clean Ag(110). Heating the crystal to 250 K results in the desorption of all molecularly bound furan from the surface, leaving hydrogen-deficient furan rings bound to the surface. The vibrational spectrum following the 254 K anneal on the O-predosed surface clearly shows that the out-of-plane modes are markedly less intense relative to the in-plane modes when compared to furan

(23) Stuve, E. M.; Madix, R. J.; Sexton, B. A. *Surf. Sci.* **1982**, *119*, 279.
(24) Stuve, E. M.; Madix, R. J.; Sexton, B. A. *Surf. Sci.* **1981**, *111*, 11.

on the clean surface. It therefore appears that the intermediates formed by hydrogen abstracted from furan on the O-predosed surface are tilted more toward the surface normal than furan on the clean surface. This ring tilt is most likely attributable to the formation of a bond between the hydrogen-deficient carbon and the surface.

Discussion

Both the TPRS and EELS clearly show that the first step in the furan combustion pathway on Ag(110) is C–H bond activation by $O_{(a)}$. Clean Ag(110) does not react with furan, and TPD shows that furan desorbs from clean Ag(110) without reaction by 250 K. Moreover, no dihydrogen desorption is observed when furan reacts with $O_{(a)}$. Hydrogen generated from furan dehydrogenation desorbs from Ag(110) only as water. Therefore, furan dehydrogenation proceeds via C–H bond activation by adsorbed atomic oxygen. On an oxygen-precovered Ag(110) surface, water formed by the reaction with acidic molecules can desorb in two states at 240 and at 300–320 K.[24] Molecularly chemisorbed water ($H_2O_{(a)}$) desorbs at 240 K; water evolution near 300 K is a reaction product of surface hydroxyl disproportionation:[24]

$$2OH_{(a)} \rightarrow H_2O_{(g)} + O_{(a)} \quad (5)$$

Because water evolution occurs primarily at 300 K and not at 240 K, water produced during the reaction of furan and $O_{(a)}$ is the result of hydroxyl disproportionation. The lack of any chemisorbed water evolution at 240 K confirms that furan is not a strong enough gas-phase acid for $OH_{(a)}$ to activate furan C–H bonds, unlike acetylene (ΔH_{acid} = 377.8 kcal/mol[25]) which is much more acidic than furan and reacts with $OH_{(a)}$ on Ag(110) to form chemisorbed water.[19]

EELS spectra provide evidence that C–H bond activation is the first step toward combustion and occurs without significant rearrangement of the furan ring. The EELS spectrum of the surface annealed to 254 K (Figure 4) clearly indicates the emergence of an O–H stretching mode and the retention of all furan ring skeletal modes, indicating that the furan ring remains intact after hydrogen extraction. Moreover, there is an observed kinetic isotope effect for hydroxyl formation. EELS experiments of furan-h_4 show that $OH_{(a)}$ groups are formed by 200 K, whereas experiments with furan-d_4 show that no $OD_{(a)}$ groups are formed at or below 200 K but are formed by 250 K. This pronounced kinetic isotope effect proves that the rate-limiting step for hydrogen extraction is hydrogen transfer to $O_{(a)}$ and not a rearrangement of the furan ring.

Initially it is surprising that $O_{(a)}$ activates furan C–H bonds. Furan, like benzene, is aromatic, yet benzene C–H bonds are not activated by adsorbed atomic oxygen on Ag(110). The reactivity of furan to adsorbed atomic oxygen can be attributed to the high gas-phase acidity (ΔH_{acid}) of furan. Because ΔH_{acid} for furan is less than that of water (388[12] and 395 kcal/mol, respectively), furan is predicted to undergo an acid–base reaction with adsorbed oxygen.[1] In addition, experiments show that propylene, which has a gas-phase acidity of 392 kcal/mol[8], and hence is less acidic than furan, readily reacts with atomic oxygen on Ag(110).[26] Benzene does not react because it is a much weaker gas-phase acid (ΔH_{acid} = 401 kcal/mol[9]). The homolytic bond dissociation energy of benzene is 111 kcal/mol,[27] but that for furan does not appear to have been measured.

Unfortunately, the results do not reveal which hydrogen of furan is first abstracted by $O_{(a)}$. Experiments on the gas-phase acidity of furan suggest that hydrogens in the α-position are three times as likely to react with OH^- as hydrogens in the β-position.[12] Even though this is strong evidence for preferential proton loss from carbons closest to the ring oxygen, conclusive evidence requires TPRS experiments using very expensive, selectively deuterated furan isotopes.

(25) Ervin, K. M.; Gronert, S.; Barlow, S. E.; et al. *J. Am. Chem. Soc.* **1990**, *112*, 5750.
(26) Barteau, M. A.; Madix, R. J. *J. Am. Chem. Soc.* **1983**, *105*, 344.
(27) McMillan, D. F.; Golden, D. M. *Ann. Rev. Phys. Chem.* **1982**, *33*, 493.

Table II. Calculated Valence Electron Density for Furan

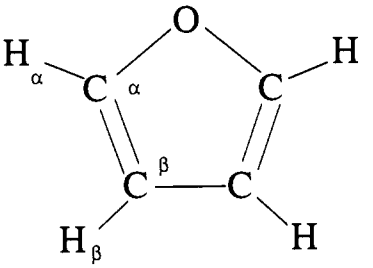

atom	MNDO/3[28]	Hartree–Fock[28]	CNDO[29]
O	6.311	6.381	6.081
C_α	3.771	3.984	3.950
C_β	4.108	4.230	4.066
H_α	0.992	0.812	0.967
H_β	0.973	0.784	0.976

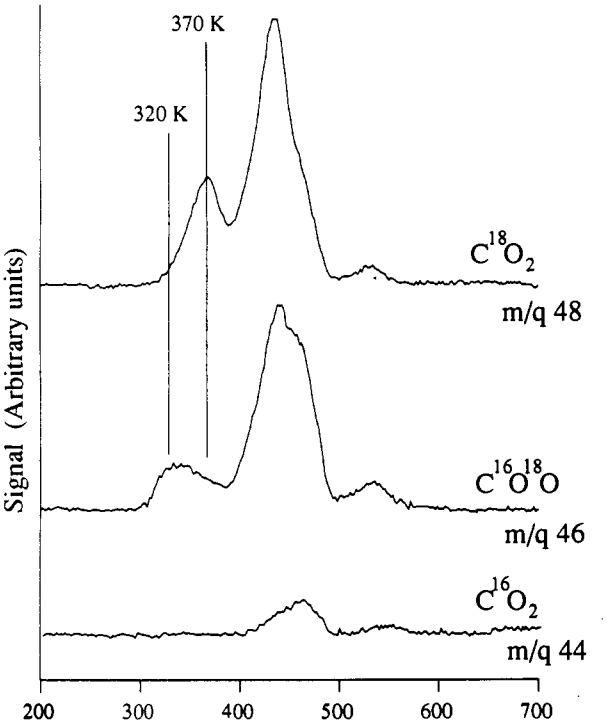

Figure 5. TPRS spectra of CO_2 isotopes for $^{18}O_{(a)}$. All three traces are shown at the same scale.

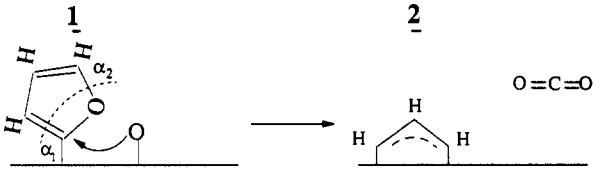

Figure 6. Possible mechanism for oxygen attack at the furanyl α-carbon at 308 K.

TPRS experiments with $^{18}O_{(a)}$ and furan clearly show that the second step in furan combustion is surface oxygen attack at the electron-deficient α-carbon. MNDO/3,[28] CNDO,[29] and ab initio Hartree–Fock[28] calculations predict valence electron density to be concentrated at the ring oxygen and deficient at the α-carbon (Table II). The electronegative ring oxygen withdraws electron density from the α-carbon. A similar distribution in electron density would be expected for α-furanyl bound to silver. Figure

(28) Defina, J. A.; Andrews, P. R. *Int. J. Quantum Chem.* **1980**, *18*, 797.
(29) Iten, P. X.; Hofmann, A. A.; Eugster, C. H. *Helv. Chim. Acta* **1978**, *61*, 430.

5 shows TPRS traces for all possible isotopes of CO_2 ($C^{18}O_2$ (m/q 48), $C^{18}O^{16}O$ (m/q 46), and $C^{16}O_2$ (m/q 44)) originating from the reaction of $C_4H_4{}^{16}O$ with $^{18}O_{(a)}$. The first isotope of carbon dioxide to appear is $C^{18}O^{16}O$ at 308 K; each CO_2 contains a ring oxygen and an oxygen from the surface. A possible reaction mechanism is illustrated in Figure 6. Although TPRS experiments do not clarify which α-carbon is attacked, adsorbed oxygen most likely attacks the proton-deficient α-carbon which is closest to the surface, particularly if this intermediate is tilted up from the surface. Attack at the α-carbon farthest from the surface is mitigated by two factors: (1) the EELS experiments suggest that after proton extraction the furan ring tilts toward the surface normal, sterically inhibiting oxygen attack, and (2) CO_2 formation from the α_2-carbon requires attack by two $O_{(a)}$, the first to extract the remaining α_2-hydrogen and the second to react with the α_2-carbon.

After attacking the α_1-carbon, the subsequent C_3H_3 fragment is attacked by surface oxygen to form $H_2{}^{18}O$ and $C^{18}O_2$, as shown by the m/q 48 peak at 370 K. The peak at 370 K, however, does not account for the complete combustion of all furan molecules attacked at 320 K. For complete furan combustion, the ratio of $C^{18}O_2$ to $C^{18}O^{16}O$ must be 3:1, whereas peak areas of the 320 and 370 K peaks yield a ratio of only 2:1. It is possible that further hydrogen abstraction by $^{18}O_{(a)}$ leads to the formation of more stable surface-bound intermediates.

Indeed, further scavenging by adsorbed oxygen occurs above 380 K, and there is no longer preferential attack at the α-carbon. There is a dramatic increase in both $C^{18}O_2$ and $C^{18}O^{16}O$ evolution, and $C^{16}O_2$ forms as well, implying that oxygen originating from furan skeletal fragments is free to scavenge surface carbon. [Although it may be argued that ^{16}O originates from an impurity in the $^{18}O_2$ dose or is the result of ^{18}O exchange with subsurface ^{16}O, TPRS of 0.25 mL of ^{18}O on Ag(110) indicates an ^{16}O impurity of only 3% and TPRS of furan on this surface shows that ^{16}O comprises 33% of the CO_2 oxygens evolving into the gas phase. This implies that 90% of the ^{16}O originates from the furan ring.] Desorption of all three isotopes of CO_2 indicates that oxygen is attacking all carbons and the integrity of the ring is destroyed.

Carbon dioxide evolution at 530 K competes with product formation, indicating that some of the hydrocarbon fragments remaining at 480 K contain oxygen. The isotopic abundance in the CO_2 formed indicates that all of the furan fragments do *not* combust to CO_2 and H_2O. The relative concentration of ^{18}O to ^{16}O in CO_2 for complete combustion of furan is 7:1. The ratio determined by experiment was only 3:1, a difference which cannot be attributed to the 3% ^{16}O impurity. Clearly the amount of oxygen preadsorbed was insufficient to completely oxidize furan to CO_2 and H_2O. In fact, oxygen scavenging decays by 490 K due to exhaustion of the $O_{(a)}$ supply and not to a lack of hydrocarbon fragments, as confirmed by oxygen titration of the residue. The lack of an O–M stretch in EELS spectra of surfaces flashed to 480 K confirms that if $O_{(a)}$ exists, it is in amounts too small for EELS detection. Integrations of TPRS data indicate that only 0.005 mL of $O_{(a)}$ participates in CO_2 evolution concurrent with partial oxidation products. In addition, no recombinative O_2 desorption occurs at 590 K.

High-temperature furan production most likely forms from the rehydrogenation of a furan ring that survives oxygen scavenging. The furan molecule does not incorporate surface oxygen into the ring, as evidenced by the absence of a parent ion mass shift in the ^{18}O TPRS experiments. Furan formation by the recombination of hydrocarbon fragments without incorporation of a surface oxygen seems unlikely. Therefore, we suggest that the ring giving rise to the furan at 520–550 K most likely remains intact throughout the scavenging process.

Bifuran can be formed by a simple recombination of adsorbed furanyls. Bifuran has been formed from metal salts, as in the following electrophilic substitution reaction of furan in aqueous Pd(II):[30]

$$2\text{furan} + \text{Pd(II)} \rightarrow \text{bifuran} + \text{Pd(0)} + 2\text{H}^+ \qquad (6)$$

(30) Kozhnevnikov, I. V. *React. Kinet. Catal. Lett.* **1976**, *4*, 451.

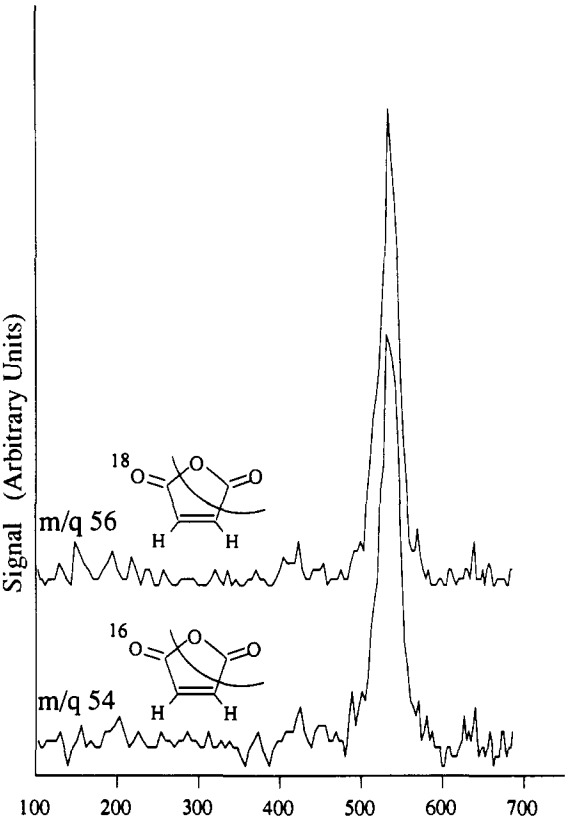

Figure 7. TPRS of m/q 54 (furan ring oxygen) and m/q 56 (surface oxygen) to determine the relative population of wing oxygens in maleic anhydride.

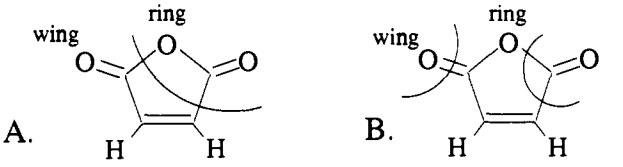

Figure 8. Possible maleic anhydride cracking patterns that give rise to m/q 54.

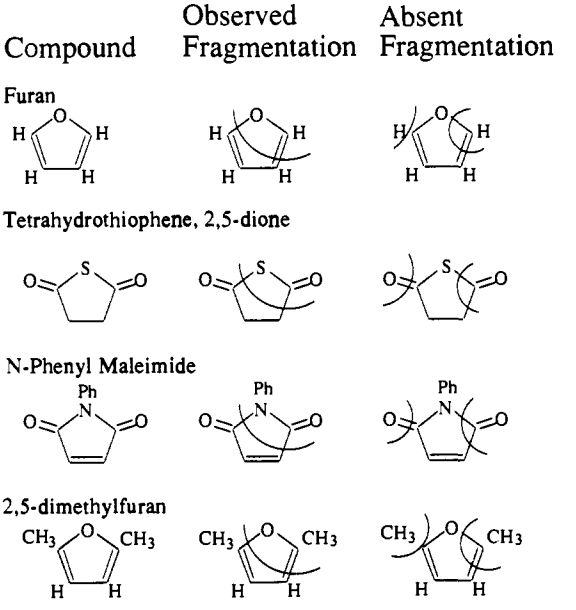

Figure 9. Published cracking pattern for compounds similar to maleic anhydride.[20]

An analogous reaction is possible for oxygen-precovered Ag(110), where oxygen abstracts a proton and a Ag–furanyl complex is formed. As in the case of furan, no surface oxygen incorporation

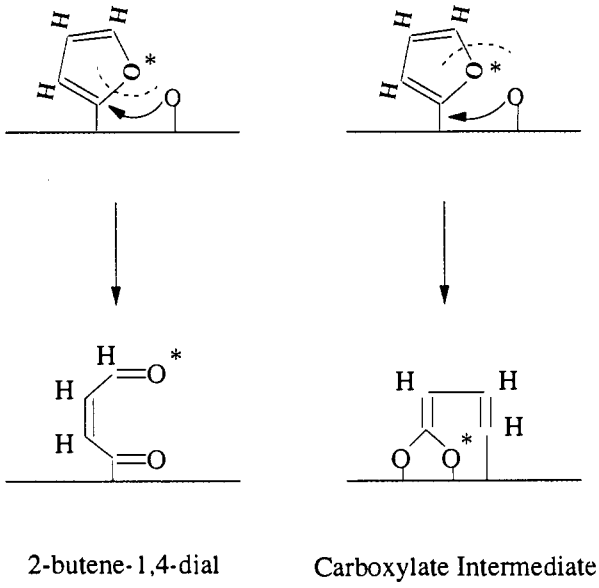

Figure 10. Possible ring opening mechanisms by $O_{(a)}$ attack at the α-carbon.

into the bifuran is observed, and the furan rings most likely remained intact throughout oxygen scavenging. The presence of bifuran is strong supporting evidence for the intermediate **1** (Figure 6).

Benzene production can be explained by the cycloaddition of the two C_3H_3 fragments **2**. The proposed reaction (Figure 6) of oxygen with adsorbed furanyls to eliminate CO_2 leaves an unstable C_3H_3 fragment. At low temperatures, surface oxygen readily attacks this fragment, but at 530 K, when surface oxygen concentrations are low, two C_3H_3 fragments may combine to form benzene. Although there is no direct proof of this mechanism, it is consistent with our observations.

Unlike the formation of high-temperature furan or bifuran, maleic anhydride is formed via intermediates that involve cleaving the furan ring. TPRS analysis of maleic anhydride cracking fractions for ^{18}O experiments show that the oxygen originating in the furan ring is not located in the ring but on the wing (Figure 7). The parent ion mass shift for maleic anhydride with ^{18}O addition clearly shows that two surface oxygens are incorporated into maleic anhydride. The position of the surface oxygens added to furan to form maleic anhydride was determined by monitoring m/q 54 and 56 during ^{18}O TPRS experiments. Maleic anhydride is expected to fragment to form m/q 54 as shown in Figure 8A. The alternative fragment yielding m/q 54 that contains the ring oxygen and not a wing oxygen (Figure 8B) is improbable for two reasons. First, in order to fragment to give a ring oxygen in m/q 54, the ionizing electron must cleave three bonds: an isolated carbon–oxygen double bond and contiguous carbon–carbon and carbon–oxygen single bonds. Only two single bonds are cleaved to form m/q 54 with a wing oxygen: a carbon–carbon and a carbon–oxygen bond. Second, published cracking fractions of analogous compounds show that furan, tetrahydrothiophene-2,5-dione, *N*-phenylmaleimide, and 2,5-dimethylfuran all fragment in analogous patterns that indicate that the oxygen in the m/q 54 fragment of maleic anhydride is a wing oxygen (Figure 9). We therefore take m/q 54 or 56 evolved at 530 K to be indicative of ^{16}O and ^{18}O in the wing position in maleic anhydride.

The reaction of $C_4H_4{}^{16}O$ with ^{18}O yields maleic anhydride exhibiting both m/q 54 and 56 with the same intensity (Figure 7); ^{18}O and ^{16}O each occupy a wing position. The oxygen originating in the furan ring moves to a wing position, and the two oxygens originally bound to the surface are located both on the wing and in the ring of maleic anhydride. It cannot be argued that wing ^{16}O is the result of scavenging and that the ring oxygen is that of the original furan because the parent ion mass shifts for ^{18}O TPRS experiments clearly show that maleic anhydride incorporates two ^{18}Os. If there is additional $^{16}O_{(a)}$ incorporation into the product, it is below the noise level of the mass spectrometer.

The mechanism for maleic anhydride formation must result in movement of the furan ring oxygen into one of the wing positions of maleic anhydride and must therefore involve ring opening. As discussed previously, the second step in furan combustion appears to be oxygen attack at the α-position to yield CO_2 and a C_3H_3 fragment. A possible competing reaction to CO_2 formation is ring opening to form either a dial or a carboxylate intermediate (Figure 10). EELS spectra of a surface annealed to 322 K (Figure 4), at which CO_2 has been formed only by oxygen attack at the α-position of furan, show a loss at 2820 and 1670 cm^{-1} in addition to losses expected for furanyl. The vibration at 2820 cm^{-1} could be the aldehyde C–H stretch of the dial intermediate and the one at 1670 cm^{-1} the C=O stretch. In fact, 2-butenedial has vibrational modes at 2800 and 1695 cm^{-1}; other modes of 2-butenedial, 2950, 1250, and 860 cm^{-1},[31] are present in the EELS

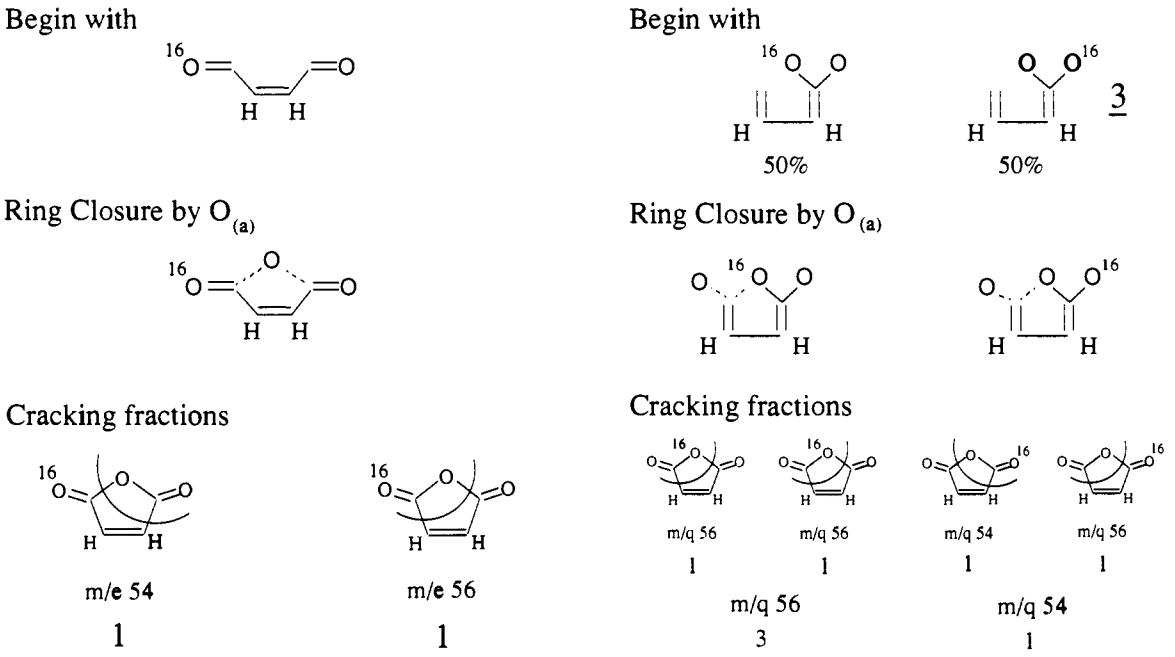

Figure 11. Schematic oxygen distribution for maleic anhydride formation formed via dial and carboxylate intermediates.

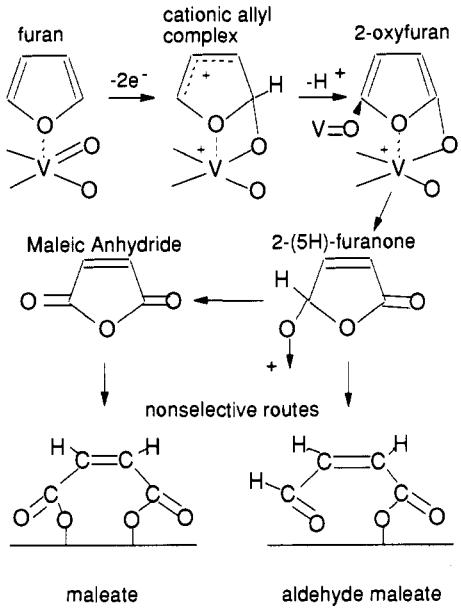

Figure 12. Proposed mechanism for maleic anhydride production from furan over a VPO catalyst.[13]

spectra at 322 K but may also be attributed to furanyl. In support of the carboxylate intermediate, the 1670-cm^{-1} mode could be the ν_{as}(OCO), which is consistent with that observed for formate on Ag(110).[32] The 2820-cm^{-1} mode, however, is not consistent with a carboxylate intermediate, but this vibration may be due to another hydrocarbon fragment. It may also be argued that the 1670-cm^{-1} mode is a ν(C=C) stretch. The EELS spectra, therefore, are somewhat ambiguous with respect to which intermediate leads to maleic anhydride production.

However, only the dial intermediate can place the ring oxygen exclusively on the wing upon formation of maleic anhydride (Figure 11). For the carboxylate intermediate, assuming that both oxygens in the carboxylate group react equivalently, oxygen which originated in the furan ring is expected to be on the wing only one time out of four. Only if there is a strict stereospecific difference in the two oxygens such that the oxygen originating from the surface always ends up in the ring (3) can the oxygen isotope distribution agree with experiments. Such a stringent stereospecific mechanism seems unlikely. To make maleic anhydride from the dial requires the removal of the aldehyde hydrogen followed by ring closure to incorporate surface oxygen, thereby always placing the original furan ring oxygen in a wing position. Precedence for ring closure by surface oxygen on Ag(110) has been established previously in the conversion of butadiene to 2,5-dihydrofuran.[7] Ring closure has also been established on Pd(111) with the cyclotrimerization of acetylene to benzene,[33] the formation of furan from $O_{(a)}$ and acetylene,[34] and the formation of thiophene from $S_{(a)}$ and acetylene.[35] In addition, butenedial has recently been proposed as an important intermediate in one of three reaction channels for the production of maleic anhydride from 1,3-butadiene over V_2O_5 catalysts;[36] ring closure is presumably one of the steps in the reaction pathway. Although experimental data do not prove that the dial intermediate exists or leads to maleic anhydride formation, the involvement of this intermediate is consistent with both EELS and isotope experiments.

The proposed mechanism of maleic anhydride production from furan on Ag(110) via ring opening contrasts with proposed mechanisms for the same reaction over a VPO catalyst. Over an alumina-supported VPO catalyst, maleic anhydride is produced via a 2(5*H*)-furanone intermediate and ring opening results in product decomposition (Figure 12).[13] On Ag(110), ring opening appears to be *required* for maleic anhydride formation. The complexity of the mechanism for maleic anhydride formation on Ag(110) may account for the low yield of maleic anhydride, because combustion of the ring-opened intermediate will compete with ring closure to form maleic anhydride.

Conclusions

Furan reacts with active oxygen on Ag(110) to form CO_2, H_2O, and small amounts of the partially oxidized products maleic anhydride, bifuran, and benzene. The first step in furan combustion is C–H bond activation by $O_{(a)}$, as predicted by the relatively high gas-phase acidity of furan. The second step in furan oxidation is surface oxygen attack of the α-carbon at 308 K to yield CO_2 and C_3H_3. A competing mechanism appears to be ring opening, yielding an oxygen-containing hydrocarbon intermediate which rearranges to maleic anhydride. This reaction sequence contrasts with mechanisms proposed for maleic anhydride production from furan over VPO catalysts, which predict that the furan ring remains intact throughout the reaction process.

Acknowledgment. We gratefully acknowledge the National Science Foundation for their support through NSF grant CTS-9005135-02.

(31) Schuster, D. I.; Eriksen, J. *J. Org. Chem.* **1979**, *44*, 4254.
(32) Sexton, B. A.; Madix, R. J. *Surf. Sci.* **1981**, *105*, 177.
(33) Tysoe, W. T.; Nyberg, G. L.; Lambert, R. M. *J. Chem. Soc., Chem. Commun.* **1983**, 623.
(34) Ormerod, R. M.; Lambert, R. M. *Catal. Lett.* **1990**, *6*, 121.
(35) Gentle, T. M.; Tsai, C. T.; Walley, K. P.; Gellman, A. J. *Catal. Lett.* **1989**, *2*, 19.
(36) Hönicke, D. *J. Catal.* **1987**, *105*, 10.